frontiers | Frontiers in Physics

BRIEF RESEARCH REPORT
published: 03 May 2022
doi: 10.3389/fphy.2022.912141

Scattering Cancellation Coating Composed of Periodical Subwavelength Structures

Weiwei Kan, Cong Tian and Yikai Chen*

School of Science, MIIT Key Laboratory of Semiconductor Microstructure and Quantum Sensing, Nanjing University of Science and Technology, Nanjing, China

We propose to cancel the scattered wave using two layers of periodical subwavelength structures by coating the scattering object with the designed composite material. As a demonstration, it is possible to obtain such scattering cancellation effect for a fiber optical nanoprobe, and fabricate the coating layers by simply etching cylinders or doping elements in silicon/SOI wafer. The required quasistatic parameters of the coating material are homogeneous and isotropic. The simulation results show that the 632.8 nm TE polarized light travels through the coated fiber optical nanoprobe with the wavefront undisturbed, and serve as evidence of the effectiveness of the designed invisibility coating. The proposed scattering cancellation scheme could be useful in non-invasive probing applications at visible and near-infrared wavelengths.

Keywords: scattering cancellation, invisibility, non-invasive probing, effective medium, metamaterial

OPEN ACCESS

Edited by:
Yu-Gui Peng,
Huazhong University of Science and Technology, China

Reviewed by:
Shen Yaxi,
Hong Kong University of Science and Technology, Hong Kong, SAR China
Zi-Lan Deng,
Jinan University, China

****Correspondence:***
Weiwei Kan
kan@njust.edu.cn

Specialty section:
This article was submitted to Physical Acoustics and Ultrasonics, a section of the journal Frontiers in Physics

Received: *04 April 2022*
Accepted: *19 April 2022*
Published: *03 May 2022*

Citation:
Kan W, Tian C and Chen Y (2022) Scattering Cancellation Coating Composed of Periodical Subwavelength Structures. Front. Phys. 10:912141. doi: 10.3389/fphy.2022.912141

INTRODUCTION

Invisibility cloak has drawn lots of attention in recent years [1–11]. Invisibility effects are usually generated with absorbing screens for eliminating the backscattering or reflection from objects. Recently, due to the possibility of cancellation or reduction of the scattered wave from the scattering object, and the potential significance in non-invasive probing/sensing applications [12–14], invisibility cloaking based on metamaterials become a hot topic.

For designing the invisibility devices, the parameter distribution is usually obtained with the technique of coordinate transformation [5, 6] or scattering cancellation [15–17]. The transformation technique often requires singular dielectric parameters or anisotropic parameters [2–6], that are difficult to implement in practice. Although the recent development of metamaterial make the nontrivial material with uncommon parameters possible to fabricate in real world [18–22], and some invisibility designs based on coordinate trasformation, such as carpet cloak or illusion cloak, have been demonstrated in laboratories [9–11], the ideal omnidirectional invisibility cloak with broad working frequency bandwidth still challenges the current fabrication technologies, especially in optical frequencies [8].

To overcome the difficulty in the invisibility design with simple parameter distributions, transparent coatings based on scattering cancellation have been proposed in the field of electromagnetics, optics and acoustics [16, 23], showing how this technique bring invisibility cloak into reality by coating the scattering object with layers of metamaterial. Although this technique is initially proposed to generate the effect of optical invisibility [13], the experimental realizations are demonstrated in the field of electromagnetics [13, 24, 25] and acoustics [14, 17]. The difficulty of achieving plasmonic material in optical frequencies impedes the development of optical invisibility coatings. To our best knowledge, a feasible implementing scheme to achieve

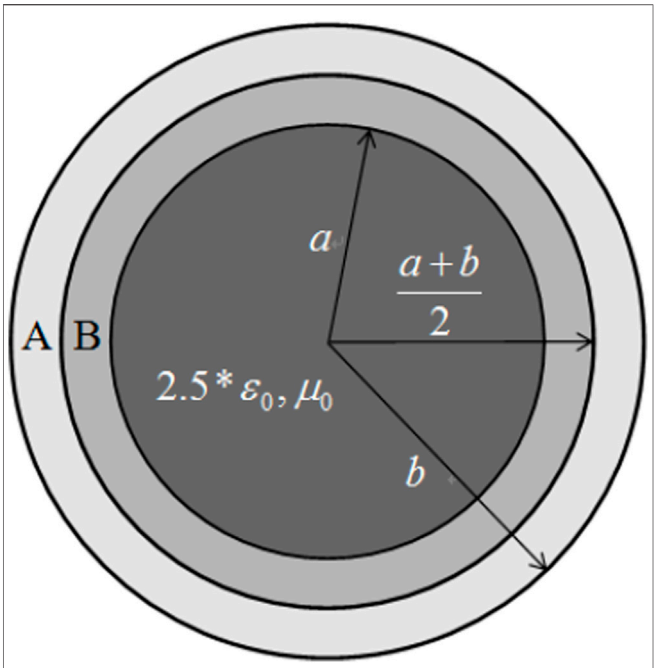

FIGURE 1 | Schematic diagram of the model. The core cylinder is the fiber optical nanoprobe to be cloaked. The cloak is composed of the two layers A and B with different optical parameters. a = 201.43 nm, and b = 322.28 nm.

omnidirectional and broadband invisibility with low loss materials remains challenging and still needs to be put forward.

In this paper, we present the design of the invisibility coating composed of two layers of metamaterial, to address the abovementioned problems in the existing devices. The scattering cross section of a concentric cylindrical system are derived and written as a function of the component material parameter. The scattering cross section is minimized with optimized parameter distribution, i.e., the materials parameters for the coating layers are determined by searching for the minimal value of the derived scattering cross section of the modeled system, chosen as the objective function of the optimization algorithm. The resulting values of the constituent parameters are different from the previous plasmonic-type coatings with much larger permittivity than air, and can be feasibly implemented by etching in silicon wafer and SOI wafer. The resulting device could be low loss compared with the devices composed of metallic material or negative-index metamaterials.

We consider an simplified fiber optical nanoprobe, i.e., an infinitely long cylindrical object of radius a, with isotropic and homogeneous parameter distribution of permittivity 2.5 ε_0 and permeability μ_0, where ε_0 and μ_0 are permittivity and permeability of air. As shown in **Figure 1**, the nanoprobe is wrapped with the bilayer concentric cylindrical coating which forms the invisibility cloak to be further designed, and illuminated by a TE polarized optical plane wave. Both the layers A and B have the same thickness of $(b-a)/2$. In the following, we use the scattering cancellation method to obtain the optical parameters of the layers, which will further be implemented with metamaterials.

As the incident wave is TE polarization mode with the electric field vector perpendicular to the cross-section of the concentric cylinder, then the electric field can be mathematically regarded as a scalar field in the plane perpendicular to the vector. Firstly, we consider a two-boundary model, i.e., the cylinder only coated by one layer with the thickness of h. The wave field in the background medium, in the coating layer and in the fiber can be respectively expanded with Bessel or Hankel series as

$$E_0 = E_{0,inc} + E_{0,scr} = \sum_n \alpha_{0,n} J_n(k_0 r) e^{in\theta} + \sum_n R_{1,n} \alpha_{0,n} H_n^{(1)}(k_0 r) e^{in\theta}, \tag{1}$$

$$\begin{aligned} E_1 &= E_{1,sta} + E_{1,f} \\ &= \sum_n S_{1,n} \alpha_{0,n} J_n(k_1 r) e^{in\theta} + \sum_n F_{1,n} \alpha_{0,n} H_n^{(1)}(k_1 r) e^{in\theta}, \end{aligned} \tag{2}$$

$$E_2 = E_{2,trs} = \sum_n T_{1,n} \alpha_{0,n} J_n(k_0 r) e^{in\theta}, \tag{3}$$

where $E_{0,inc}$, $E_{0,scr}$ is the electric field of the incident wave and scattering wave filed in the background medium, $E_{1,sta}$, $E_{1,f}$ is the standing field and outgoing cylindrical wave in the coating layer, and $E_{2,trs}$ is the field in the region inside the hidden nanoprobe.

The boundary condition equations at the interfaces of the layers are:

$$\begin{cases} E_{inc}|_{r=a,a+h} + E_{scr}|_{r=a,a+h} = E_{tra}|_{r=a,a+h} \\ \vec{n} \cdot \frac{1}{\mu_0} (\nabla E_{inc}|_{r=a,a+h}) \vec{n} \cdot \frac{1}{\mu_0} (\nabla E_{scr}|_{r=a,a+h}) = \vec{n} \cdot \frac{1}{\mu_1} (\nabla E_{tra}|_{r=a,a+h}) \end{cases} \tag{4}$$

Substituting **Eqs. 1–3** into **Eq. 4**, the coefficients $R_{1,n}$ of the single-layer structure that give the scattering field of the system can be obtained. Our model, however, is made up of concentric cylinders with more coating layers. For the goal of calculating the wave field scattered by this more complicated system, the layer B can be regarded as an effective boundary, and the coefficients $R_{1,n}$, $T_{1,n}$ can be regarded as the reflection and transmission coefficients at this effective boundary, then the bilayer model become an effective single-layer structure and the corresponding scattering problem can be calculated using **Eqs 1–4**. This process turns the calculation of the multilayer scattering problem into a recursive progress, starting from the innermost layer, to the outermost layer. When the scattering problem of the whole system are solved, we obtain the total scattering coefficients $R_{j,n}$ and define the scattering cross section of the cylinder with j coating layers in the far field as

$$\sigma = \frac{2}{\pi k_0} \int_0^{2\pi} \left| \sum_n R_{j,n} \exp\left(in\left(\theta - \frac{\pi}{2} \right) \right) \right|^2 \mathrm{d}\theta, \tag{5}$$

The smaller the scattering cross section is, the better stealth effect one gets.

Based on the previous equations, the scattering cross section of the system shown in **Figure 1** can be regarded as a function of the material parameters of layers A and B. By taking the scattering cross section as the objective function of

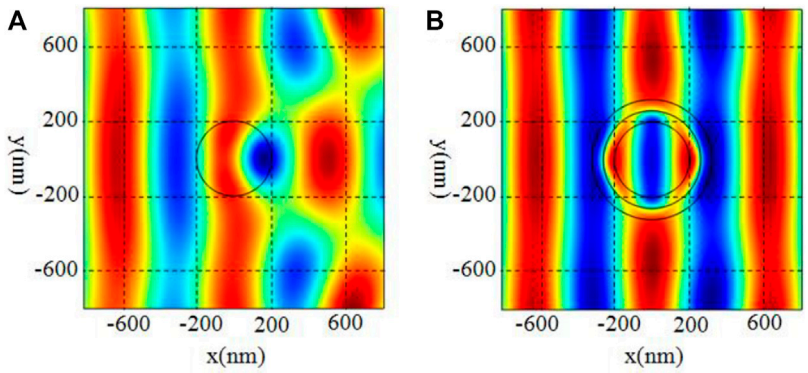

FIGURE 2 | (Color online) The electric field excited by the 632.8 nm plane optical wave **(A)** without and **(B)** with the cloak.

the standard genetic algorithm, and searching in the realizable parameter space for the best stealth effect, the optimum material parameters of the coating layers for constructing the scattering-cancellation type cloak are found. The optimized constitutive material parameters that can make the nanoprobe undetectable to the detecting signals are $5.1\varepsilon_0$, μ_0 and $11.5\varepsilon_0$, μ_0 for layers A and B respectively, which are different with the plasmonic cloak, where effective parameters of the coating layers are far smaller than those in air [15]. To demonstrate the performance of this cloak, the electric fields excited by the plane optical wave with wavelength of 632.8 nm for the nanoprobe without and with the cloak are calculated using the above recursive method by taking $S_{j,n}$ and $F_{j,n}$ in **Eq 1** into account, and shown in **Figures 2A,B** respectively. For the case without the cloak, the back scattering and shadow area can be clearly observed in **Figure 2A**. But in **Figure 2B** it can be seen that, under the protecting of the coating layers, the scattering from the nanoprobe and the corresponding shadow area are both cancelled, with the field for plane wave in free space recovered. By applying this cloak, the scattering cross section is reduced to 4.2 percent of the case without cloak.

In order to realize the effective parameters, the subwavelength structures designed by the effective medium theory (EMT) are periodically arranged as shown in **Figure 3**. As the required parameters are isotropic, the inserted structures are chosen as cylinders and arranged in square lattice with lattice constant of d. The radius of the embedded cylinder is r, which should be small enough to meet the requirement of EMT [26]. The important configurations that eventually determine the effective features of the composite material are the parameters of the component material and the ratio of the cylinder radius to the lattice constant. For constructing layer A with a relative permittivity 5.1, silicon cylinders are chosen and properly arranged in air. And layer B with permittivity $11.5\varepsilon_0$ is achieved by drilling cylindrical holes on silicon wafer. The illustration of unit cells for both layers is shown in **Figure 3A**, and the effective parameters can be precisely modulated by tuning the filling ratio of silicon. The effective parameters can be retrieved by studying the reflection and transmission properties when plane wave incident to the unit cells. According to this well-established retrieving method [26], the effective parameters when changing the filling ratio are calculated and shown in **Figure 3B**. As expected, for layer A, with the increase of r/d, the relative permittivity increases monotonously, while for layer B decreases. For both cases, permeability remains the same. According to **Figure 3B**, the required effective parameters for layer A and B can be achieved at $r/d = 0.31$ and $r/d = 0.29$ respectively.

Once the ratio of the embedded cylindrical radius to the size of the unit is determined, the size of the unit cells could be the designed by considering the geometry of our cloaking layers. In order to ensure the validation of effective medium approximation, the dimension of the unit cell should be small enough, but smaller nanoscale structures are more difficult to fabricate. After balancing the invisibility effect and the difficulty in practical fabrication, we choose the dimension of the unit cell as 16 nm, which is more than 20 times smaller than the wavelength and sufficiently ensure the validation of effective medium approximation. The silicon (gray) microstructures for layers A and B are shown in **Figures 3C,D**. For checking the broadband performance of the unit cell, we have studied its effective parameters between the range of 500–800 nm. The relative effective permittivity and permeability for layers A and B is given in **Figures 3E,F** by red (solid), and blue (dashed). By comparing the results with the ideal parameters (red dashed), it can be seen that in the long wavelength range from 600 to 800 nm, all the effective parameters agree well with the ideal values, which promise the good broadband performance of the unit cell and the resulting cloak. For all the cases, the relative permeability is approximately around one. As the dimension of the unit cell is enough small, all the obtained effective parameters approximately remains constant near 632.8 nm, suggesting the subwavelength structures are effective in broadband, while the value of permittivity begins to increase gradually at around 530 nm due to the dispersion effect of the lattices and the silicon material. This dispersion effect is caused by the multiple scattering among the cylinders as the wavelength

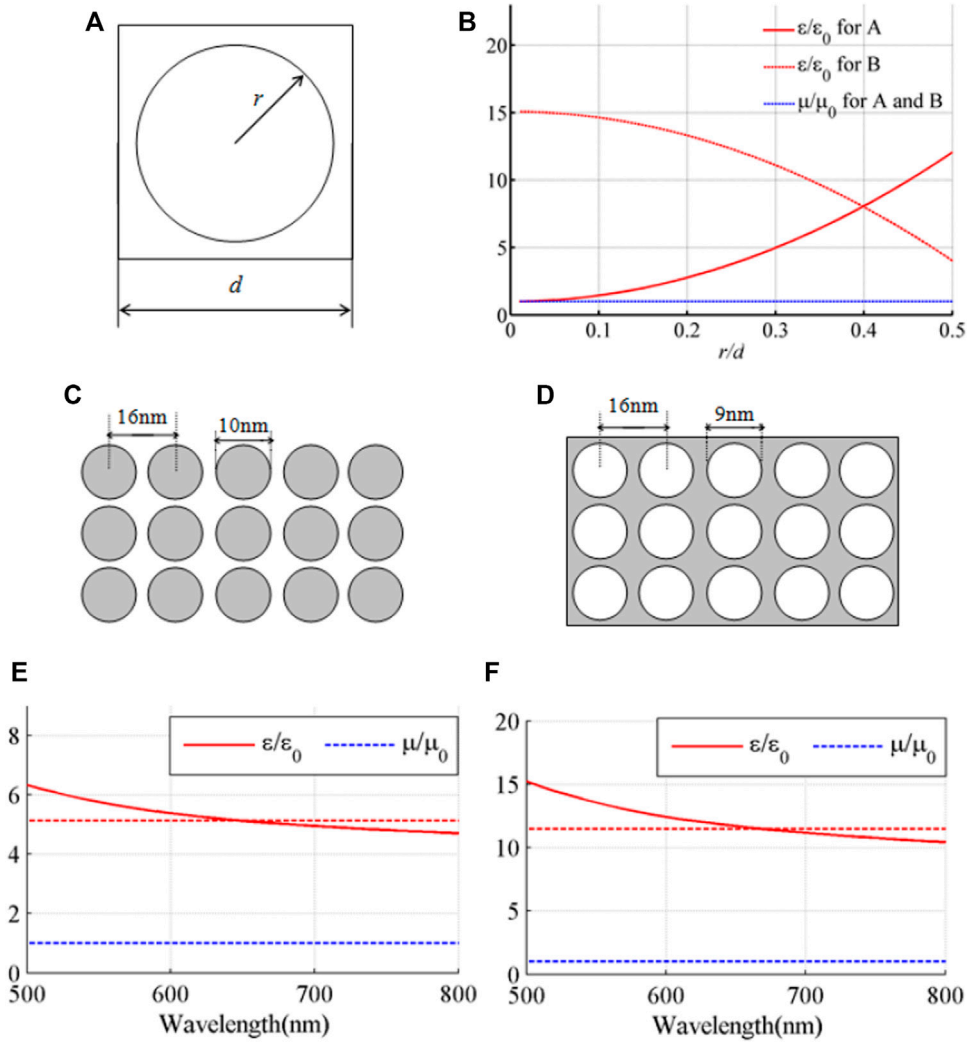

FIGURE 3 | (Color online) **(A)** Illustration of unit cells for both layers. **(B)** The effective permittivity for layers A (red solid) and B (red dashed) and the relative permeability (blue dashed) **(C–D)** Illustration of the silicon (gray) microstructures for layers A **(C)** and B **(D) (E–F)** The effective parameters for layers A **(E)** and B **(F)** when changing the incident wavelength. Red (blue) data: relative permittivity (effective relative permeability). The dashed red lines give the ideal values of relative permittivity for the two layers according to the scattering cancellation method.

become smaller and the requirement of EMT is gradually deviated. Better invisibility effects, broader bandwidth and lower loss can be achieved with smaller unit structures, but the fabrication of such nanostructures would be difficult. All the conclusions agree well with the EMT.

In order to demonstrated the effectiveness of the design, the electric field when the 632.8 nm optical wave incidents to the nanoprobe coated by the two metamaterial layers is calculated and shown in **Figure 4A**. It can be observed that the plane wave field pattern is well recovered as if the wave is traveling in free space, and the field is nearly the same with the results given in **Figure 2B**. The scattering field from the nanoprobe is suppressed under the protecting of the coating layers as shown in **Figure 4B**, and loss is hardly observed as the structures are deep subwavelength and multiple scattering among them is very week. For showing the robustness of the design, we also give the performances of the coatings composed of unit cells with different sizes in **Figures 4C,D** respectively. The stealth effects of the corresponding cloaks when the cell dimension is 32 and 63 nm are also acceptable, but the coating with the 16 nm unit size generate the best invisibility effect. The results confirm the above conclusions that smaller unit cells will generate better stealth effects, as requirement of the effective medium theory is better satisfied when the unit structures are deeper subwavelength, but further deceasing the dimensions may lead to more stringent requirements for the manufacturing process. The integral is done over the intensity of scattering field in the area surrounding layer A. The performance of the device is quantitatively verified by calculating the scattering cross section when changing the incident wavelength from 500–800 nm. The scattering cross section is generally

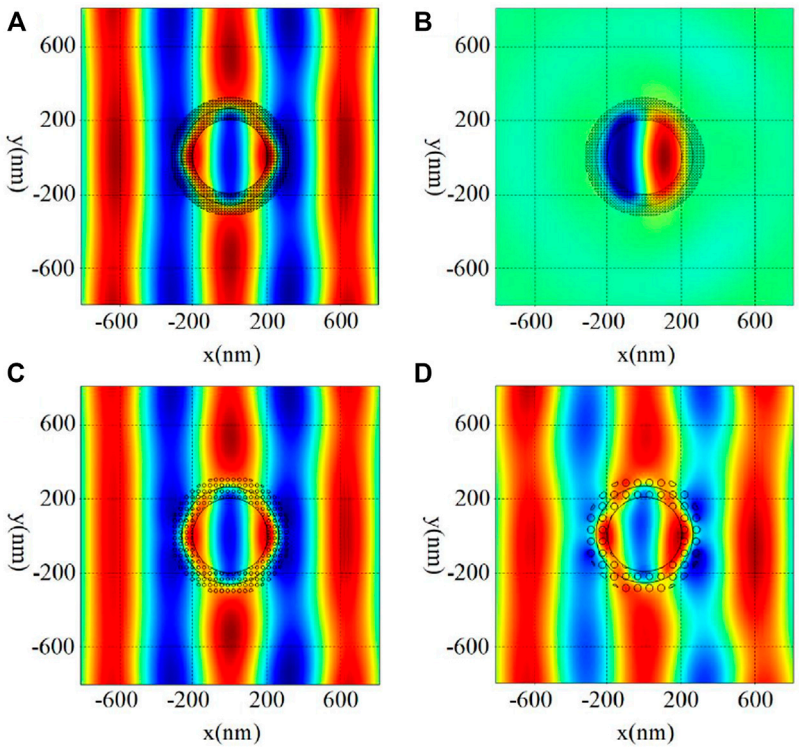

FIGURE 4 | (Color online) **(A,C–D)** The electric field excited by the 632.8 nm plane optical wave for the cloak constructed by the subwavelength structures with cell dimension of 16 nm **(A)**, 32 nm **(C)** and 63 nm **(D)**. **(B)** The scattering field from the nanoprobe which is under the protecting of the coating layers constructed by the subwavelength structures with cell dimension of 16 nm.

decreased by the proposed coating layers to less than 0.2 for most of the wavelength from 600–680 nm, except at the wavelength of 653 nm, where additional scattering is generated by a whispering gallery mode.

In conclusion, we proposed the scattering cancellation type invisibility coating for realizing non-invasive probing with a fiber optical nanoprobe. The coating layers can be feasibly constructed by etching in silicon wafer and SOI wafer. The effective parameters of the composite material are precisely modulated in order to meet the requirements of the scattering cancellation. Stealth effects are obtained at the wavelength of around 532 nm with the scattering cross section decreased to less than 0.2. The results show that for the given configuration, the structures are still effective even when the wavelength is 600 nm, and the scattering cross section remains a small value in the whole investigated frequency range. The ability of guiding optical waves around objects like the nanoprobe makes this design potentially useful for versatile wave manipulation applications.

DATA AVAILABILITY STATEMENT

The original contributions presented in the study are included in the article/Supplementary Material, further inquiries can be directed to the corresponding author.

AUTHOR CONTRIBUTIONS

WK: Methodology, writing, reviewing and editing. CT: Programming, methodology, writing, reviewing and editing. YC: Methodology, reviewing and editing.

FUNDING

This work was supported by National Natural Science Foundation of China (Grant No. 11974186), Natural Science Foundation of Jiangsu Province (No. BK BK20200070).

REFERENCES

1. Zhou C, Cheng Y, Li J-y.B, Liu X-j. Reconstructed Imaging of Acoustic Cloak Using Time-Lapse Reversal Method. *Appl. Phys. Express* (2014) 7:087301. doi:10.7567/apex.7.087301
2. Kan W, García-Chocano VM, Cervera F, Liang B, Zou X-y., Yin L-l., et al. Broadband Acoustic Cloaking within an Arbitrary Hard Cavity. *Phys Rev Appl* (2015) 3:064019. doi:10.1103/physrevapplied.3.064019
3. Kan W, Shen Z. Ultra-transparent Media with Anisotropic Mass Density for Broadband Acoustic Invisibility. *Appl. Phys. Lett.* (2017) 111:223501. doi:10.1063/1.5002741

4. Lai Y, Chen H, Zhang Z-Q, Chan C. Complementary Media Invisibility Cloak that Cloaks Objects at a Distance outside the Cloaking Shell. *Phys. Rev. Lett.* (2009) 102. doi:10.1103/physrevlett.102.093901
5. Pendry JB, Schurig D, Smith DR. Controlling Electromagnetic Fields. *Science* (2006) 312:1780–2. doi:10.1126/science.1125907
6. Zhu X, Liang B, Kan W, Zou X, Cheng J. Acoustic Cloaking by a Superlens with Single-Negative Materials. *Phys. Rev. Lett.* (2011) 106:014301. doi:10.1103/physrevlett.106.014301
7. Popa B-I, Zigoneanu L, Cummer SA. Experimental Acoustic Ground Cloak in Air. *Phys. Rev. Lett.* (2011) 106:253901. doi:10.1103/physrevlett.106.253901
8. Wu K, Cheng Q, Ping Wang G. Fourier Analysis: from Cloaking to Imaging. *J. Opt.* (2016) 18:044001. doi:10.1088/2040-8978/18/4/044001
9. Zhang BL, Luo YA, Liu XG, Barbastathis G. Macroscopic Invisibility Cloak for Visible Light. *Phys. Rev. Lett.* (2011) 106:033901. doi:10.1103/physrevlett.106.033901
10. Zhang X, Gharghi M, Gladden C, Zentgraf T, Liu YM, Yin XB, et al. A Carpet Cloak For Visible Light. *Nano Lett* (2011) 11:2825.
11. Zigoneanu L, Popa B-I, Cummer SA. Three-dimensional Broadband Omnidirectional Acoustic Ground Cloak. *Nat Mater* (2014) 13:352–5. doi:10.1038/nmat3901
12. Zhu X, Liang B, Kan W, Peng Y, Cheng J. Deep-Subwavelength-Scale Directional Sensing Based on Highly Localized Dipolar Mie Resonances. *Phys Rev Appl* (2016) 5. doi:10.1103/physrevapplied.5.054015
13. Alù A, Engheta N. Cloaking a Sensor. *Phys. Rev. Lett.* (2009) 102:233901. doi:10.1103/physrevlett.102.233901
14. Guild MD, Alù A, Haberman MR. Cloaking of an Acoustic Sensor Using Scattering Cancellation. *Appl. Phys. Lett.* (2014) 105:023510. doi:10.1063/1.4890614
15. Alu A, Engheta N. Achieving Transparency with Plasmonic and Metamaterial Coatings. *Phys Rev E Stat Nonlin Soft Matter Phys* (2005) 72:016623. doi:10.1103/physreve.72.016623
16. Guild MD, Haberman MR, Alù A. Plasmonic-type Acoustic Cloak Made of a Bilaminate Shell. *Phys. Rev. B* (2012) 86:104302. doi:10.1103/physrevb.86.104302
17. Sanchis L, García-Chocano VM, Llopis-Pontiveros R, Climente A, Martínez-Pastor J, Cervera F, et al. Three-Dimensional Axisymmetric Cloak Based on the Cancellation of Acoustic Scattering from a Sphere. *Phys. Rev. Lett.* (2013) 110:124301. doi:10.1103/physrevlett.110.124301
18. Kan W, Liang B, Tian C, Shen Z, Cheng J. A Broadband Low-Reflection Bending Waveguide for Airborne Sound. *Appl. Phys. Lett.* (2017) 110:253502. doi:10.1063/1.4986510
19. García-Chocano VM, Christensen J, Sánchez-Dehesa J. Negative Refraction and Energy Funneling by Hyperbolic Materials: An Experimental Demonstration in Acoustics. *Phys. Rev. Lett.* (2014) 112:144301. doi:10.1103/physrevlett.112.144301
20. García-Chocano VM, Graciá-Salgado R, Torrent D, Cervera F, Sánchez-Dehesa J. Quasi-two-dimensional Acoustic Metamaterial with Negative Bulk Modulus. *Phys Rev B* (2012) 85:184102. doi:10.1103/PhysRevB.85.184102
21. Zhu X, Li K, Zhang P, Zhu J, Zhang J, Tian C, et al. Implementation of Dispersion-free Slow Acoustic Wave Propagation and Phase Engineering with Helical-Structured Metamaterials. *Nat Commun* (2016) 7:11731. doi:10.1038/ncomms11731
22. Li Y, Shen C, Xie Y, Li J, Wang W, Cummer SA, et al. Tunable Asymmetric Transmission via Lossy Acoustic Metasurfaces. *Phys Rev Lett* (2017) 119:035501. doi:10.1103/physrevlett.119.035501
23. Guild MD, Haberman MR, Alù A. Cancellation of the Acoustic Field Scattered from an Elastic Sphere Using Periodic Isotropic Elastic Layers. *J. Acoust. Soc. Am.* (2010) 128:2374. doi:10.1121/1.3508436
24. Edwards B, Alù A, Silveirinha MG, Engheta N. Experimental Verification of Plasmonic Cloaking at Microwave Frequencies with Metamaterials. *Phys. Rev. Lett.* (2009) 103:153901. doi:10.1103/physrevlett.103.153901
25. Xiang N, Cheng Q, Chen HB, Zhao J, Jiang WX, Ma HF, et al. Bifunctional Metasurface for Electromagnetic Cloaking and Illusion. *Appl Phys Express* (2015) 8:092601. doi:10.7567/apex.8.092601
26. Fokin V, Ambati M, Sun C, Zhang X. Method for Retrieving Effective Properties of Locally Resonant Acoustic Metamaterials. *Phys. Rev. B* (2007) 76:144302. doi:10.1103/physrevb.76.144302

Conflict of Interest: The authors declare that the research was conducted in the absence of any commercial or financial relationships that could be construed as a potential conflict of interest.